

# Analytical Model to Estimate Ride Pooling Traffic Impacts by Using the Macroscopic Fundamental Diagram

Transportation Research Record  
2022, Vol. 2676(4) 697–709  
© National Academy of Sciences:  
Transportation Research Board 2022



Article reuse guidelines:  
sagepub.com/journals-permissions  
DOI: 10.1177/03611981211064892  
journals.sagepub.com/home/trr



Aledia Bilali<sup>1</sup> , Ulrich Fastenrath<sup>1</sup>, and Klaus Bogenberger<sup>2</sup> 

## Abstract

Ride pooling services are considered as a customer-centric mode of transportation, but, at the same time, an environmentally friendly one, because of the expected positive impacts on traffic congestion. This paper presents an analytical model that can estimate the traffic impacts of ride pooling on a city by using a previously developed shareability model, which captures the percentage of shared trips in an area, and the existence of a macroscopic fundamental diagram for the network of consideration. Moreover, the analytical model presented also investigates the impact that improving the average velocity of a city has on further increasing the percentage of shared trips in an operation area. The model is validated by means of microscopic traffic simulations for a ride pooling service operating in the city of Munich, Germany, where private vehicle trips are substituted with pooled vehicle trips for different penetration rates of the service. The results show that the average velocity in the city can be increased by up to 20% for the scenario when all private vehicle trips are substituted with pooled vehicle trips; however, the improvement is lower for smaller penetration rates of ride pooling. The operators and cities can use this study to quickly estimate the traffic impacts of introducing a ride pooling service in a certain area and for a certain set of service quality parameters.

## Keywords

analytical modeling, on-demand mobility, ride pooling, shareability, traffic impact, macroscopic fundamental diagram, planning and analysis, transportation network modeling

Our cities are experiencing growth in population every year, which contributes to increased traffic demand. The use of private vehicles—even though convenient—is not sustainable, considering the large amount of parking space and street capacity that is required as a result of an average occupancy of only 1.3 passengers per vehicle (1). From the other side, traditional public transportation is typically an efficient and environmentally friendly mode of transportation; however, it may not be very attractive for customers because of the lack of convenience and flexibility as a result of fixed line and schedule and a limited area of coverage.

The extended availability of smartphones and data accessibility have made possible the emergence of ride pooling services. These services offer a user-centric and sustainable mobility option for the customer, which can reduce the vehicle kilometers traveled in the system because of sharing of trips with similar trajectories (2–4).

However, an effective ride pooling service depends largely on the customers' readiness to use it, which is affected by individual choices and on the attributes of the service. The service attributes which affect customers the most are travel time, waiting time and service cost, and the lower they are, the higher is the attractiveness of the service (5).

From the operators' perspective, the percentage of shared trips in an area, called shareability, influences the profitability of the service, and therefore plays an important role in deciding whether to offer a pooling service in

<sup>1</sup>BMW AG, Munich, Germany

<sup>2</sup>Traffic Engineering and Control, Technical University of Munich, Munich, Germany

## Corresponding Author:

Aledia Bilali, aledia.bilali@tum.de

an area or not. Santi et al. examined shareability in a city via simulations by using the concept of shareability networks (6). To generalize the calculation of shareability for different cities, Tachet et al. established a mathematical model, in which shareability depends on city parameters (average speed and surface of the operating area) and service attributes (detour time) and tested it for different cities (7). Their model was extended by Bilali et al. to capture the additional influence of maximum waiting time, boarding time, and reservation time, and the impact that the modeling details have on shareability, showing that, in particular, the choice of the optimization objective has a high effect on shareability (8–10).

The before-mentioned studies derived shareability without considering the traffic impact of ride pooling. Therefore, average velocity—a commonly used measure of traffic efficiency—is assumed to be constant in space and time in these models. However, by introducing a ride pooling service in a city, the number of vehicles on the roads will decrease, thereby increasing the average velocity in the network. As the velocity is in turn an input for the shareability model, the percentage of shared trips in an area will increase even further. This effect is noted as second-order effect of velocity on shareability and its basic idea is illustrated in Bilali et al. for a synthetic grid network (11). In this paper, the concept of this second-order effect will be explored for a real city network and a more realistic analytical model capturing traffic effects of ride pooling.

The benefits of ride pooling, focusing on a particular city, have been investigated a lot by researchers. Alonso Mora et al. showed that 98% of taxi trips in New York city currently catered for by 13,000 taxis, can be substituted by a fleet of only 3,000 pooled vehicles, reducing the mean travel distance in the system (2). A study for the city of Prague, Czech Republic, substituting private vehicle trips with pooled trips, demonstrated that, when using ride pooling, vehicle kilometers will decrease to 60% of the current state (3). A similar study was performed for the city of Munich, Germany, and the authors argue that the benefits of pooling are seen only after a certain penetration rate of the service, for which the saved travel kilometers resulting from shared trips are higher than the empty vehicle trips generated to pick-up customers (4).

All of the above studies investigate only the impact from the pooled vehicle fleet and indirectly check the traffic impacts by calculating the vehicle kilometers in the system, without examining the interaction with the other vehicles that are present in the network. These studies are performed using agent-based simulations, which, even though providing a good estimation of the vehicle kilometers in the system, are specific for a particular city and require a large amount of input data. Therefore, a

generalization for different city types is difficult. Albeit the traffic impacts of ride pooling are not directly investigated in these studies (as, for instance, would be the case if the agent-based simulation were to be coupled with a microscopic traffic simulation), the computational time needed for these simulations is still very high and rises with increasing problem size. Therefore, it is difficult to simulate high-demand pooling states, and it is even more difficult and time demanding to investigate the direct traffic impact by integrating the agent-based simulation and microscopic traffic simulation for the pooling case.

To overcome the drawbacks of using agent-based simulations and to be able to estimate quickly the impact of ride pooling with only a little input data, this paper presents a method to derive analytically the traffic impacts of ride pooling services. The main requirement is the existence of a macroscopic fundamental diagram (MFD) for a specific city. Additionally, the influence that the improvement of average velocity in the city has on shareability is also modeled. The models presented in this paper are tested for the city of Munich using AIMSUN as a microscopic simulation environment.

## Analytical Model

This section describes a model allowing the analysis of traffic impacts of ride pooling. Firstly, an introduction to the shareability model is given, followed by a model for the reduction of vehicle trips in the road network resulting from shared trips. Subsequently, the relation between average velocity and vehicle trip generation and the modified shareability model are described. A detailed description of the model parameters can be found in Table 1.

### Shareability Model

The benefits of ride pooling are reliant on the possibility of sharing trips which have similar trajectories. The percentage of shared trips in an area is called shareability  $S$  and differs based on city parameters, service quality parameters, and the used optimization objective. The general formula defining shareability  $S$  is given by the following Equation (7–10):

$$S = 1 - \frac{1}{2(L_{sq}^{on})^3} (1 - e^{-L_{sq}^{on}}) (1 - (1 + 2L_{sq}^{on}) e^{-2L_{sq}^{on}}) \quad (1)$$

where the dimensionless quantity  $L_{sq}^{on}$  (“on” refers to online or on-demand generation of requests, and “sq” refers to the consideration of service quality parameters) depends on the pooled passenger trip generation rate per hour  $\lambda_p$ , city attributes (velocity  $v$  and surface area  $\Omega$ ), and service quality attributes (temporal deviation from the direct route or detour time  $\Delta$ , maximum waiting time

the passenger waits to be picked-up  $t^{max}$ , and boarding/ disembarking time  $t^b$ ) (8).

The calculation of shareability is based on the notion of the shareability shadow, which defines the geometric shape of where in space the origins and destinations of a trip should be to be shareable with an already existing trip, without violating the time constraints (defined by service quality parameters) (7). Depending on the relation that service quality parameters have with each other, there are two different shapes of the shareability shadow specified by Bilali et al. and, therefore, two forms of  $L_{sq}^{on}$  (8).

For  $t^{max} > \Delta - t^b$ :

$$L_{sq}^{on} = \left(\frac{v^2 \lambda_p}{\Omega}\right) (\Delta - t^b)^3 \left(\frac{2}{3\pi} + \frac{1}{\pi} \sqrt{\left(\frac{t^{max}}{\Delta - t^b}\right)^2 - 1} + \frac{1}{\pi} \left(\frac{t^{max}}{\Delta - t^b}\right)^2 \sin^{-1} \frac{\Delta - t^b}{t^{max}}\right) \quad (2)$$

and for  $t^{max} < \Delta - t^b$

$$L_{sq}^{on} = \left(\frac{v^2 \lambda_p}{\Omega}\right) (\Delta - t^b)^3 \left(\frac{2}{3\pi} + \frac{1}{2} \left(\frac{t^{max}}{\Delta - t^b}\right)^3\right). \quad (3)$$

The above equations determine the value of shareability when the optimization objective in the customer matching problem is to maximize the percentage of trips which will be shared (8). However, using the objective of maximizing the percentage of shared trips does not necessarily mean that the distance traveled is minimized. To maximize the percentage of shared trips, the pooling algorithm might decide about sharing of the trips (when the time constraints allow it) just for the sake of achieving maximum percentage of shared trips, even though it might be more effective in relation to saved vehicle kilometers to serve the customers one after the other (10).

As the optimization objective to minimize vehicle kilometers traveled is more favorable to improve the traffic conditions, it is the one selected in this study. The shareability for this optimization objective is given by a prediction model defined by Bilali et al. and inspired by Santi et al. and shown in Equation 4 (6, 10). This form of equation also describes statistically the natural combinatorial effects of particle bonding processes in biochemistry. To use this prediction model, the results of the shareability values derived by means of simulations for a base scenario referring to a certain set of service quality parameters are needed. Therefore, by fitting the simulated shareability data to the form of shareability equation given by Equation 4, the parameters  $n$  and  $k$  are defined. To calculate the shareability for another set of service quality parameters, the parameters  $n$  and  $k$  are kept the same and the impact of the new service quality

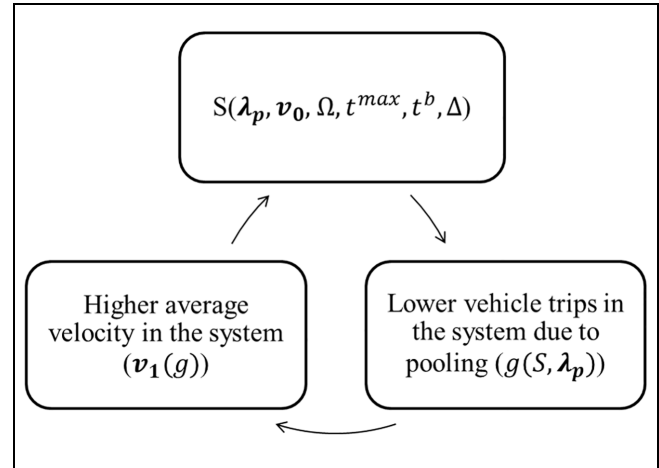


Figure 1. Additional effect of average velocity on shareability.

parameters is reflected in the  $L_{sq}^{on}$  quantity. For the case when the optimization objective is to minimize the vehicle kilometers traveled, this prediction model is tested in Bilali et al. with data from an agent-based simulation, and the results showed that the model provides a good estimation of the shareability values for this optimization objective (10). Therefore, similar to Bilali et al., the shareability in this study for the case when the optimization objective is to minimize the vehicle kilometers traveled is calculated by using Equation 4 (10).

$$S_{n,k}(L_{sq}^{on}(v, \Delta, t^b, t^{max})) = \frac{kL_{sq}^{onn}}{(1 + kL_{sq}^{onn})} \quad (4)$$

This shareability model returns the percentage of shared passenger trips in an area, while assuming that the average velocity in the city  $v = v_0$  remains constant. However, for a certain pooled passenger trip generation rate per hour  $\lambda_p$ , the number of total vehicle trips per hour in the system  $g$  is reduced based on the percentage of trips that are shareable  $S(v_0)$ . And, as for a lower number of vehicles in the system, the average velocity in the system gets higher and a change in average velocity  $v_1$  is encountered, which should be reflected in the shareability model and additionally increase the shareability value  $S(v_1)$ . These interactions (recently considered in the literature by Bilali et al., and Lehe and Pandey) are described by a loop diagram in Figure 1 (11, 12). Therefore, the analytical model developed in this study considers the synergetic effects that increased pooling rate and average network velocity have on each other. In the following sections, the reduced number of vehicle trips in the system as a result of ride pooling will be defined, followed by the description of an analytical model that relates average velocity with the vehicle trips generated per hour in the city.

Table 1. Model Parameters

Constant parameters	Math notation	Description	Value	Unit
Surface area	$\Omega$	Area of the operation	221	km <sup>2</sup>
Network length	$L$	Total length of the network	2,450	km
Velocity at capacity	$v_c$	Average velocity when the network is at capacity	39.2	km/h
Flow at capacity	$q_c$	Average flow when the network is at capacity	457	vph
Average velocity for morning peak	$v_o$	Initial average velocity for the morning peak for the base scenario	39.2	km/h
Parabola's parameter	$a$	Parameter of the parabolic function found by data fitting	0.062	na
Average vehicle trip length with origin and destination in the area	$l_{od}$	Average vehicle trip length of trips that have the origin and destination in the area of operation	5.16	km
Average vehicle trip length with only origin in the area	$l_o$	Average vehicle trip length of trips that have only the origin in the area of operation	17.5	km
Average vehicle trip length with only destination in the area	$l_d$	Average vehicle trip length of trips that have only the destination in the area of operation	17.5	km
% of $l_o$ within the area of operation	$p_o$	% of $l_o$ within the area of operation	51	%
% of $l_p$ within the area of operation	$p_d$	% of $l_p$ within the area of operation	46	%
Detour time	$\Delta$	Time delay caused by detour	5	minutes
Maximum waiting time	$t^{max}$	Maximum time waiting to be picked up	5	minutes
Boarding/disembarking time	$t^b$	Time needed to board/disembark the vehicle	0	minutes
Vehicle occupancy	$\Phi$	Maximum $\Phi$ passengers can share the trip at the same time	2	passengers
Variable parameters	Math notation	Description	Relation	Unit
Average velocity	$v$	Average velocity in the network at a certain time of day	na	km/h
Average flow	$q$	Average flow in the network at a certain time of day	na	vph
Average density	$k$	Average density in the network at a certain time of day	na	vehicles per km
Shareability	$S$	Probability of finding the matching trip in a network to share ride	Equations 1–4	%
Ride pooling penetration rate	$p$	Fraction of pooled passenger trips/total passenger trips ( $p = \lambda_p/\lambda$ )	0, 5, 25, 50, 75, 100	%
The original private vehicle matrix	$A_0$	The original private vehicle matrix	na	na
Lone-passenger trip generation	$\lambda_o$	Lone-passenger trips generated in an hour and performed by private vehicles	$(1-p)A_0$	passenger trip per hour
Pooled passenger trip generation	$\lambda_p$	Pooled passenger trips requests generated in an hour and performed by pooling service	$pA_0$	passenger trip per hour
Lone-vehicle trip generation	$g_o$	Lone-vehicle trips generated in an hour by private vehicles	$g_o = \lambda_o$	vehicle trips per hour
Pooled vehicle trip generation	$g_p$	Pooled vehicle trips generated in an hour by pooling service	$g_p \rightarrow$ Equation 5	vehicle trips per hour
Total vehicle trip generation in the operation area	$g_{od}+g$	Total vehicle trips generated in an hour in the service area of pooling service.	$g = g_o + g_p$	vehicle trips per hour
Vehicle trips generation with only origin in the area	$g_o$	Vehicle trips generation that have only the origin in the area of operation	na	vehicle trips per hour
Vehicle trips generation with only destination in the area	$g_d$	Vehicle trips generation that have only the destination in the area of operation	na	vehicle trips per hour

Note: vph = vehicles per hour; na = not applicable.

### Vehicle Trip Reduction Model

A distinction is made between passenger trips generation rate  $\lambda$ , for trips requested by the customers, and vehicle trips generation rate  $g$ , for vehicle trips occurring in the street, which can serve more than one customer simultaneously. For simplicity, it is assumed that private vehicle trips will be replaced by pooled vehicle trips. However, as the implementation of ride pooling in a city will be gradual, there will be passengers who will still use their private vehicles to travel alone and there will also be passengers who will use the ride pooling service. Therefore, the total passenger trips generated per hour in the area  $\lambda$  is divided into lone-passenger trips  $\lambda_a$  and pooled passenger trips  $\lambda_p$ . The number of lone-vehicle trips generated per hour in the system  $g_a$  will be the same as the hourly number of lone-passenger trips  $\lambda_a$  ( $g_a = \lambda_a$ ), as there is only one person per vehicle. As the pooled passenger trips  $\lambda_p$  can be shared with each other, the number of pooled vehicle trips generated per hour in the system,  $g_p$ , depends on the percentage of shared trips in the operating area (shareability)  $S$  and the occupancy of the vehicles  $\Phi$  in the form given by Equation 5. This indicates that, for a shareability value higher than zero, the hourly pooled vehicle trips  $g_p$  will be lower than the hourly pooled passenger trips  $\lambda_p$ , as there can be more than one passenger served simultaneously by vehicles. This equation gives a lower bound for the reduction of pooled vehicle kilometers traveled, as it does not consider the empty pick-up trips or the reallocation trips and assumes that all the passenger trips which are shared have the same origin and destination. Therefore, by using this assumption, this model underestimates the total number of vehicle trips generated per hour in the system and, thereby, the positive traffic impacts in reality might be lower than the ones predicted by the analytical model.

$$g_p = \lambda_p(1 - S) + \frac{S\lambda_p}{\Phi} \quad (5)$$

Therefore, the total number of vehicle trips per hour in the system  $g$  includes the lone-vehicle trips  $g_a$  and the pooled vehicle trips  $g_p$  and is given by Equation 6, where shareability  $S$  is calculated using Equations 1–4.

$$g = g_a + g_p = \lambda_a + \left( \lambda_p(1 - S) + \frac{S\lambda_p}{\Phi} \right) \quad (6)$$

This reduction in total vehicle trips in the system is expected to improve traffic conditions in the city by improving the average velocity.

### Analytical Relation of Average Velocity and Vehicle Trip Generation

As previously mentioned, reducing the number of vehicles in the system will affect the average velocity in the

city. This section will present an analytical model to capture the relation of average velocity and vehicle trip generation by exploiting the benefits of an MFD. Therefore, it will be possible to analytically derive the improvement in average velocity coming as a result of the reduction of vehicle trips in urban areas because of ride pooling.

**Macroscopic Fundamental Diagram (MFD).** MFD (or network fundamental diagram) defines the functional form of the relation between average velocity, traffic flow  $q$  (vehicles per hour [vph]) and traffic density  $k$  (vehicles per kilometer). The relation between these parameters was firstly developed for motorway segments by using roadside sensors (13). Researchers discovered that a similar relation exists also for urban networks. Godfrey proposed an MFD for a town center road network and empirically calibrated it (14). A summary of the MFDs for different networks can be found in Cassidy et al. (15). A functional form of the MFD for urban areas, relating travel production (vehicle-meters) with accumulation (vehicles), was defined by Daganzo, and validated by Geroliminis and Daganzo (16, 17). Since then, the MFD was developed for different urban areas by using detector or floating car data or analytically (17–20). MFD has also been exploited in ride hailing studies, which do not consider ride pooling, as a background in dynamic modeling of urban traffic modeling to develop a revenue maximization platform (21). It was also used as a means for dynamic modeling and control of a network taxi dispatch system (22).

The functional form of MFD is also going to be exploited in this study and used as a basis for defining the relationship between average velocity and vehicle trip generation in a network. The MFD for this study is derived by means of simulations. For each time interval,  $I$ , the average velocity  $v_e^i$  and flow  $q_e^i$  for each edge in the network is obtained, and the weighted average velocity and flow in the network are defined using the below equations, as proposed by Geroliminis and Daganzo, where  $l_e$  is the length of each edge  $e$  (17):

$$v^i = \frac{\sum_{e \in E} v_e^i l_e}{\sum_{e \in E} l_e} \quad (7)$$

$$q^i = \frac{\sum_{e \in E} q_e^i l_e}{\sum_{e \in E} l_e} \quad (8)$$

As the relation of flow and velocity resembles a parabola, to connect these two parameters analytically, a parabolic function is defined in the form given by Equation 9, where the vertex of the parabola is  $V(q_c, v_c)$ ,  $v_c$  and  $q_c$  are velocity and flow when the network is at capacity, and  $a$  is a parameter which will be defined by fitting the data points to this function. A parabolic form

of the MFD is also noticed in Geroliminis and Daganzo, and Ramezani and Nourinejad (17, 22).

$$(v - v_c)^2 = 4a(q - q_c) \tag{9}$$

**Analytical Vehicle Trips in a Network Based on MFD.** Firstly, a simple method to define the traffic density of a network analytically will be described. It is assumed that a ride pooling service will be operated in an area defined by a boundary, as illustrated in Figure 2. Within this area, there are three different types of trip to be considered: (1) the ones that have the origin and destination within the area, (2) the ones that have the origin in the area and the destination outside, (3) the ones that have the destination in the area and the origin outside, and (4) the trips that have both origin and destination outside the operation area but pass through it. The first type of trip includes the lone-vehicle trips and the potential pooled vehicle trips. The second and third types of trip are the ones that comprise what will be called here “background traffic” in the network as they are going to be there regardless of the impact of the ride pooling service in vehicle trip reduction, as the impact that might come from parking in the boundary of the area of service and continuing the trip with ride pooling service is neglected in this study. To define the traffic density within the boundaries of this area, only the contribution of vehicle trip types (1), (2), and (3) are considered, and the contribution from type (4) is left out, as most of the cities have a highway belt to reduce transit traffic within the city.

Traffic density is defined as the number of vehicles per lane kilometer in the system. According to Little’s law the average number of vehicles in the system is equal to the average time the vehicles spend in the system multiplied by the average number of vehicles generated (23). If only the vehicles of type (1), which have both the origin and the destination within the area of operation, are considered, the traffic density  $k_{od}$  is given by Equation 10:

$$k_{od} = \frac{g_{od} l_{od}}{L} \tag{10}$$

where

$g_{od}$  is the average number of vehicle trips per hour generated inside the area (denoted by  $g$  in the Vehicle Trip Reduction Model section),

$l_{od}$  is the average vehicle trip length,

$v$  is the average velocity in the network, and

$L$  is the total network length.

For vehicle trips of type (2) and (3), which have only their origin or destination within the area, the background density  $k_b$  is given by Equation 11:

$$k_b = \frac{g_o \frac{p_o l_o}{v} + g_d \frac{p_d l_d}{v}}{L} \tag{11}$$

where

$g_o$  ( $g_d$ ) is the average number of vehicles generated which have only the origin (destination) inside the area, and

$l_o$  ( $l_d$ ) is the average vehicle trip length for this vehicle type.

As the vehicle trips of this type are only partly inside in the area,  $p_o$  and  $p_d$  give the percentage of the vehicle trip length types (2) and (3), respectively, that is, within the area of operation.

The overall network’s traffic density is the sum of the traffic density of vehicle trips type (1), (2), and (3), as illustrated in Equation 12.

$$k = k_{od} + k_b = \frac{g_{od} \frac{l_{od}}{v} + g_o \frac{p_o l_o}{v} + g_d \frac{p_d l_d}{v}}{L} \tag{12}$$

From the MFD relation,  $q = vk$  is substituted, and traffic flow  $q$  and, consequently, also the relation of flow and vehicle trips generated per hour inside the network ( $g_{od}$ ), are derived analytically by the below formulation:

$$q = \frac{g_{od} l_{od} + g_o p_o l_o + g_d p_d l_d}{L} \tag{13}$$

From Equation 13 it is possible to derive the generated number of vehicle trips of type (1), which have both the origin and destination in the operated area  $g_{od}$  (as these are the ones of interest for the ride pooling service) by Equation 14:

$$g_{od} = \frac{qL - (g_o p_o l_o + g_d p_d l_d)}{l_{od}} \tag{14}$$

By substituting  $q$  in Equation 9 of the MFD, the relation of average velocity and vehicle trips generated per hour inside the network ( $g_{od}$ ) given by Equation 15 is obtained, from which two values are obtained, depending on which state the network is: free flow state (Equation 16) or congested state (Equation 17).

$$\begin{aligned} (v - v_c)^2 &= 4a \left( \frac{g_{od} l_{od} + g_o p_o l_o + g_d p_d l_d}{L} - q_c \right) \\ &= 4a \left( \frac{(\lambda_a + (\lambda_p(1 - S) + \frac{S\lambda_p}{\Phi}))l_{od} + g_o p_o l_o + g_d p_d l_d}{L} - q_c \right) \end{aligned} \tag{15}$$

If  $v > v_c$ :

$$v = v_c + \sqrt{4a \left( \frac{g_{od} l_{od} + g_o p_o l_o + g_d p_d l_d}{L} - q_c \right)} \tag{16}$$

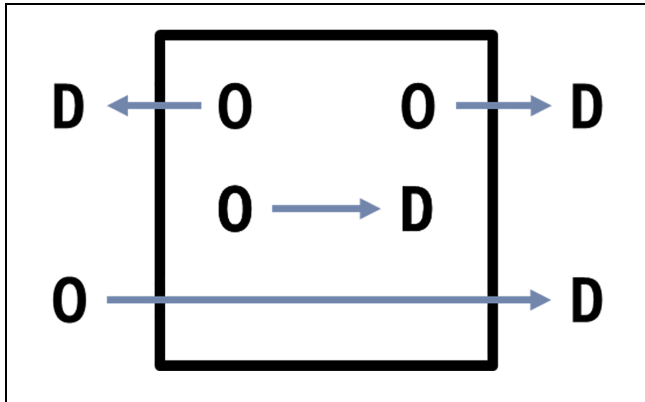


**Figure 2.** Illustration of an operating area with position of origin-destination (OD) trips.  
Note: D = destination; O = origin.

And if  $v < v_c$ :

$$v = v_c - \sqrt{4a \left( \frac{g_{od}l_{od} + g_{op}l_{o} + g_{dp}l_{d}}{L} - q_c \right)} \quad (17)$$

In this way, it is possible to derive the new average velocity in the network, only by having knowledge of the MFD and the reduced number of vehicle trips per hour resulting from pooling, calculated by Equation 6 when shareability value is known. The parabolic shape of this relation is also supported by a recent study from Ke et al. (24).

### Modified Shareability Model

By capturing the impact that ride pooling has on improving average velocity in the network, this study also captures the additional impact that the change in average velocity has on the shareability value. Therefore, this part describes the modified shareability model where, different from previous studies, velocity is considered as a dynamic parameter.

To define the modified shareability value, the dynamic velocity formulation, which depends on shareability, given in Equation 15, is substituted into the shareability Equations 2 and 3. Therefore, the modified  $L_{sq_{mod}}^{on}$  is given by the following equations:

For  $t^{max} > \Delta - t^b$

$$L_{sq_{mod}}^{on} = \left( \frac{(v(S))^2 \lambda_p}{\Omega} \right) (\Delta - t^b)^3 \left( \frac{2}{3\pi} + \frac{1}{\pi} \sqrt{\left( \frac{t^{max}}{\Delta - t^b} \right)^2 - 1} + \frac{1}{\pi} \left( \frac{t^{max}}{\Delta - t^b} \right)^2 \sin^{-1} \frac{\Delta - t^b}{t^{max}} \right) \quad (18)$$

and for  $t^{max} < \Delta - t^b$

$$L_{sq_{mod}}^{on} = \left( \frac{(v(S))^2 \lambda_p}{\Omega} \right) (\Delta - t^b)^3 \left( \frac{2}{3\pi} + \frac{1}{2} \left( \frac{t^{max}}{\Delta - t^b} \right)^3 \right). \quad (19)$$

Substituting  $L_{sq_{mod}}^{on}$  in Equation 4, which gives the shareability for the optimization objective of minimizing the vehicle kilometers traveled in the system, a non-linear equation of shareability is obtained. The Newton-Raphsod iterative method is used to solve the fixed point problem presented in Equation (25) to find the new values of the average velocity and, thereby, also the new values of modified shareability.

$$F(S) = S - \frac{kL_{sq_{mod}}^{on} n}{\left( 1 + kL_{sq_{mod}}^{on} n \right)} = 0 \quad (20)$$

The model described in this section can capture analytically the traffic impact that ride pooling has on average velocity and the improvement that it may additionally cause to the urban environment because of the additional increase of shareable trips. This implies that traffic improvement resulting from ride pooling will also be beneficial for operators to increase the chances of finding shareable trips as a result of further distances reached within the allowed detour time because of higher velocity.

## Simulation Setup

### Operating Area

To validate the developed model and investigate the traffic impact of introducing a ride pooling service, a ride pooling service in the city of Munich is considered, where private vehicle trips are substituted with pooled vehicle trips for different penetration rates of the service. The Munich network is built in the microscopic traffic simulation environment AIMSUN (26). The operating area considered (Figure 3) is located around Munich city center, similar to the one in Bilali et al. (10). Its surface is 221 km<sup>2</sup> and the network length  $L$  is 2450 km. The traffic demand in this area represents private vehicle trips for Munich (27).

To construct the MFD for this network and extract the relevant information, microscopic simulations are run for the time period from 06:00 to 24:00. To push the network to capacity, two other simulations are also run for scenarios where the private vehicle trip demand is increased by 10% and 20%, respectively. One (network average) flow-velocity data point is extracted every 10 min based on Equations 7 and 8, and it is plotted in the MFD graph.

## Scenario Setup

To test the impact of pooling for a more congested network, the traffic demand of the base scenario is selected to be 10% higher than the current demand from private vehicle trips in Munich and it is assumed that the pooling service is offered during the morning peak time from 07:00 to 10:00. The simulation for the base scenario is run, the results are extracted every 10 min, and the average velocity in the network for each time interval is obtained by using Equation 7. The average velocity for the morning peak time  $v_o$  is found to be 39.2 km/h.

To investigate the traffic impacts of a ride pooling service offered within the area of Figure 3, private vehicle trips type (1) are substituted by pooled vehicle trips for different scenarios, where the penetration rate of ride pooling service  $p = \lambda_p/\lambda$  is 0%, 5%, 25%, 50%, 75%, and 100%. The base scenario is the one where  $p = 0\%$ , meaning that all the vehicle trips in the system are not shared and are performed by private vehicles. For  $p = 100\%$ , all the private vehicle trips in the system are substituted by ride pooling vehicle trips.

To model these pooling scenarios in AIMSUN, a distinction is made between the traffic demand generated in the network from different vehicle types, and three origin–destination (OD) matrices are created: *matrix* ( $B$ ) for the background traffic (vehicle trips type [2], [3] and [4]), *matrix* ( $A$ ) for the private (lone) vehicle trips type (1) ( $g_a$ ) and *matrix* ( $P$ ) for the pooled vehicle trips type (1) ( $g_p$ ). The latter two are the ones that have both their origin and destination within the area of operation. *Matrix* ( $B$ ) representing vehicle trips which have only the origin or the destination within the area (type [2] and [3]) or only pass through the area (type [4]), does not change regardless of the reduction of pooled vehicle trips. *Matrix* ( $A$ ) for private vehicle trips type (1) and *matrix* ( $P$ ) for pooled vehicle trips will be changed depending on the selected ride pooling scenario.

It is assumed that private vehicle and ride pooling trips follow the same OD distributions and scale as the demand matrices based on  $A_0$ , the original private vehicle matrix. For each scenario considered, the value of lone-vehicle trips  $g_a$  for *matrix* ( $A$ ) of private vehicle trips is changed by using Equation 21. For *matrix* ( $P$ ) of pooled vehicle trips  $g_d$ , firstly, the pooled passenger demand  $\lambda_p$  is obtained by using Equation 22 and then the pooled vehicle trips  $g_p$  is calculated by using Equations 5 and 6, knowing the shareability value for the designed ride pooling service and the specific pooled passenger trip demand  $\lambda_p$ .

$$g_a = \lambda_a = (1 - p)A_0 \quad (21)$$

$$\lambda_p = pA_0 \quad (22)$$

For the ride pooling service selected in this study, where the optimization objective used by the operator for the matching algorithm is to minimize the vehicle kilometers traveled in the system, shareability in the area is derived by using Equations 2–4. The area of the city ( $\Omega$ ) is known and the average velocity ( $v_o$ ) is obtained from the simulation of the base scenario. The service quality attributes of detour time  $\Delta$  and maximum waiting time  $t^{max}$  are selected to be both equal to 5 min, the boarding time  $t^b$  is set to 0 for simplicity, and it is assumed that a maximum of two passengers can share the trip at the same time (vehicle occupancy  $\Phi = 2$ ).

For each scenario, one simulation is run for the morning peak time 07:00 to 10:00 and the network statistics are extracted every 10 min. Similar to the base scenario, the average velocity in the network is calculated for each time interval by using Equation 7 and then it is averaged for the morning peak time. All the model parameters and values are shown in Table 1.

## Results

### Macroscopic Fundamental Diagram (MFD) for Munich Network

The MFD for the operating area in the city of Munich is shown in Figure 4. As specified in the Scenario Setup section, the blue data points to construct this MFD were extracted from the results of three scenarios with different demand levels. The virtual queues of the vehicles waiting to get into the network are kept at minimum to control the state of the network and make sure that network gridlock, which might occur when the input flow exceeds the supply function, is not happening.

The  $x$ -axis correspond to the value of average traffic flow and the  $y$ -axis corresponds to average velocity. It is shown that the area of consideration from the Munich network is at the free flow state most of the time, while reaching the unstable state at the network's capacity during the peak times. This form of the MFD for the city of Munich is similar to the one observed in Dandl et al. (28). The high average velocity values come as a result of the large area considered, which contains city highways and arterials, where the speed limit is high. A clockwise hysteresis loop is observed for the investigated scenarios caused when the demand starts decreasing after the peak time, showing that the system does not return to the free flow state immediately if the initial congestion level in the network is high (16). Therefore, the hysteresis phenomenon in this study occurs when, for the same average flow in the network, the average velocity is higher during the congestion onset compared with its values during the congestion offset. Geroliminis and Sun show that one reason for the occurrence of this phenomenon is the





**Figure 3.** Munich operating area.

dissimilar spatial and temporal distribution of traffic congestion (29). The correlations of the loop size of the MFD, congestion heterogeneity, and network performance are further examined in Hemdan et al. (30). At the point where the traffic flow is at maximum at the MFD graph, the network is in its optimum state and the network's traffic flow at capacity  $q_c$  is derived. The corresponding velocity is the network's velocity at capacity  $v_c$ . The values of traffic flow and velocity at capacity are equal to 39.2 km/h and 457 vph, respectively. In the congestion regime, where the velocity and traffic flow are lower than the ones at capacity, the chaotic nature of traffic leads to network gridlocks, and even small disturbances effect the system; that is why the data points in this regime are widely scattered. These results are in line with previous studies, which show that, in the congestion regime, bifurcation occurs and the MFD becomes multi-valued (31).

To get a functional form for this MFD, the equation of parabola specified in Equation 15 is used. As the majority of the data points belong to the free flow state and the base scenario has data points only in this state, the data is fit to the parabolic function defined in Equation 16 for  $v > v_c$ , where the vertex of the parabola is defined by the point where the network is at capacity  $V(q_c, v_c)$ . The parameter  $a$  of the parabolic function is found to be 0.62. The fitted curve is shown by the black line in Figure 4.

### Average Velocity and Vehicle Trip Generation Relation

**Network Information.** To express the relation of average velocity and vehicle trip generation, it is necessary to extract the network information mentioned in Equation

14, namely trip lengths and percentage of the trip length inside the operating area for different vehicle trip types, for the base scenario.

To get the length of the vehicle trips type (1), (2), and (3), the centroid statistics in AIMSUN are used. The centroids within the area of operation are extracted, and the total number of vehicle trips type (1), (2), and (3), and the total kilometers traveled by each of these vehicle trip types, are calculated. By dividing the total kilometers performed by each vehicle trip type with the total number of vehicles of the respective type, the average trip length for the vehicle trips type (1), (2), and (3) is calculated to be 5.16 km, 17.5 km, and 17.5 km, correspondingly.

As vehicle trips type (2) and (3) are only partly within the area of operation, it is necessary to find the percentage of their trip length that contributes to the road network traffic within the area. Therefore, all possible paths connecting each origin with each destination are excerpted, and only the ones which start or end within the operation area are filtered. For the path that is mostly used by the vehicles, the identification numbers and lengths of the sections are obtained, and whether these sections are within or outside the area of operation is checked. The length of the trip performed within the area will be similar to the sum of the length of the sections which are situated inside the area. Dividing the vehicle trip length within the area by the total vehicle trip length returns the percentage of the vehicle trip length that is inside the operation area. In this case, the values are 51% and 46% for vehicle trips type (2) and (3), respectively.

**Average Velocity and Vehicle Trip Generation Relation.** The relation between average velocity and vehicle trip generation per hour for the vehicle trips which have both their origin and destination within the area ( $g_{od}$ ) is illustrated in Figure 5. The dark blue data points are coming from the simulation input of generated vehicle trips and the simulated average velocity in the network. For the light blue data points, the  $x$ -value showing the vehicle trips per hour is derived analytically using Equation 14, and the  $y$ -value is the simulated average velocity.

For the simulated data points, it can be seen that there are a few scattered data points, which belong to the unstable state of the network and correspond to the hysteresis shown in MFD in Figure 4. Comparing the simulated data points with the analytically derived ones, it is possible to see quite a good correlation between them, denoting that the analytical formulation for defining the generated vehicle trips in the network based on network and trip information holds for the free flow state of the network. Further investigations are, however, needed for the congested state of the network to check the validity of the model also for this state. As this is not the case for the network in this study, it is not considered.

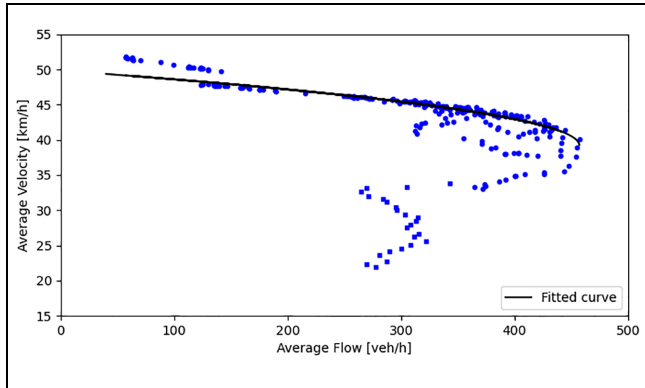


Figure 4. Macroscopic fundamental diagram (MFD) for Munich.

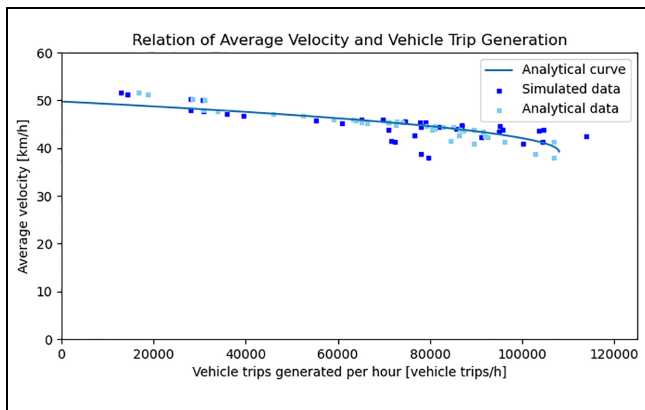


Figure 5. Relation of average velocity ( $v$ ) and vehicle trip generation ( $g_{od}$ ).

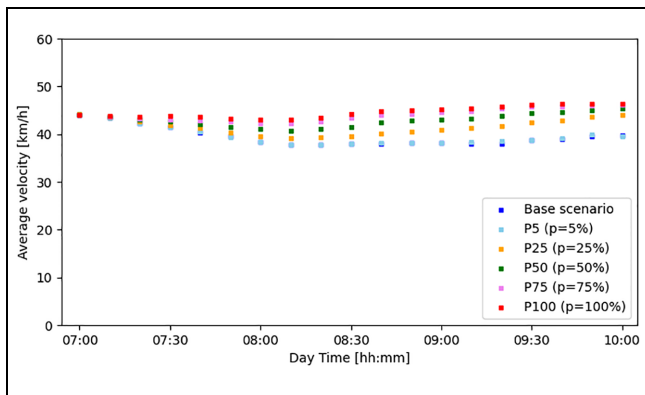


Figure 6. Average velocity for different pooling penetration rates.

The analytical function relating average velocity and vehicle trip generation ( $g_{od}$ ) using Equation 16 is illustrated by the light blue line in Figure 5. It can be noted that the analytical function fits well with both the simulated and analytical data. Deriving this relation

analytically, by having information of only trip information and the MFD relating average velocity and average flow, is quite important to define traffic impacts of ride pooling by capturing the change in average velocity if the vehicle trip generation in the network changes. As the shareability value  $S$  for the defined ride pooling system for a certain ride pooling passenger demand  $\lambda_p$  can be obtained using (Equations 1–4), it is then possible to derive the reduced number of vehicles in the street  $g_{od}$  because of pooling, based on Equation 6. By using this value as an input to this function, it is possible to calculate the new average velocity in the network. This function will be used as an input to analytically derive the additional improvement in the shareability values as a result of improved average velocity, described in the next section.

### Traffic Impacts of Ride Pooling

To investigate the traffic impacts of ride pooling service, various scenarios are designed, where the penetration rate of ride pooling service  $p$  ranges from 5% to 100%, and *matrix* ( $A$ ) of private vehicle trips and *matrix* ( $P$ ) of pooled vehicle trips are changed as specified in the Scenario Setup section.

Figure 6 depicts the average velocity every 10 min for the morning peak hour for different penetration rates of ride pooling. It is observed that, at the beginning of the morning peak, when the network is not in congested state even for the base scenario, there is no significant improvement of average velocity in the network for all the scenarios tested. When the network starts to get congested and the average velocity starts decreasing, the benefits of pooling become noticeable. This emphasizes the advantage of pooling in improving traffic condition, especially during peak times, and shows that it is possible to see higher benefits of pooling in cities with high levels of congestion.

As expected, it is shown that, the higher the penetration rate of pooling, the higher the increase in average velocity. This comes as a result of high demand for pooling, which increases the chances of finding shareable trips (shareability). Therefore, as more trips are shared, fewer vehicles are present in the road network and higher velocities are observed. Figure 7 illustrates the improvement of average velocity compared with the base scenario and shows that when the penetration rate of pooling is 100% the velocity can increase by up to 20% compared with the base scenario. For scenario P5, when the penetration is 5%, the effect of ride pooling on average velocity is quite small, indicating that when this service is introduced the effect on traffic is not expected to be seen immediately. However, with increasing market share, the positive impact of pooling will be more prominent. For instance,

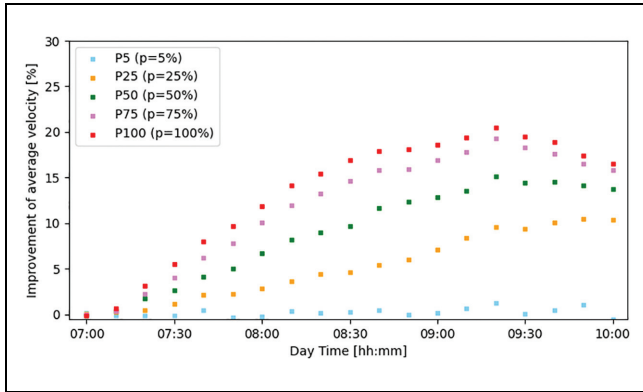


**Figure 7.** Difference in average velocity compared with the base scenario.

for scenario P25, when the penetration rate of ride pooling is 25%, the average velocity rises by up to 10% compared with the base scenario. This suggests that ride pooling services have to gain a considerable market share to profit from their positive impacts on traffic congestion.

### Modified Shareability Model

The results of the previous section show that, when private vehicle trips are substituted with ride pooling, traffic congestion is expected to improve and, therefore, the velocity will increase depending on pooled passenger demand, which effects the shareability value. Until now, velocity was considered as a constant parameter for the shareability model. Using Equations 18–20 it is possible to integrate a dynamic velocity into the shareability model and the result is illustrated in Figure 8.

The dotted gray curve shows the shareability curve for the original shareability model using the constant average velocity for the base scenario  $v_o$ , and the solid gray curve shows the modified shareability curve for a dynamic velocity. The difference between the two curves for the case study is not very big, as the average velocity was already rather high in the base scenario ( $v_o = 39.2\text{km/h}$ ) and its improvement was limited; however, an improvement of the shareability values when the velocity increases can still be seen, suggesting that this might increase additionally the chances of finding shareable trips and, thus, the average velocity in the city. The black data points in Figure 8 are the calculated shareability values considering the improvement in average velocity for the simulated scenarios with  $p$  equal to 5%, 25%, 50%, 75%, and 100%. The leftmost point represents the shareability value when  $p$  equals 5% and the rightmost point represents the shareability when  $p$  equals 100%. For each of these scenarios, the simulated shareability data points are calculated by using the new improved average velocity for the whole period of the peak hours under

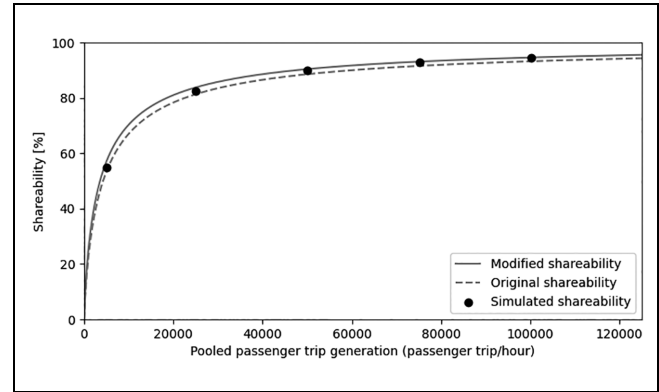


**Figure 8.** Analytical (original and modified) and simulated shareability depending on the pooled passenger trips ( $\lambda_p$ ).

consideration. These data points show how improvement in average velocity resulting from ride pooling (given by the simulation results) further increase the simulated shareability values. A very good correlation with the modified shareability model is shown for all of them, validating in this way the result of the analytical model. Even though the impact of an increased velocity on the modified shareability in the case study is small, it is nevertheless an important finding, as it implies that, for cities which are more congested than Munich, the likelihood of finding shareable trips will further increase, because of the higher possibility for improvement in average velocity.

## Conclusion

### Summary

In this study, an analytical model to investigate the impact of ride pooling on traffic efficiency was developed by using a shareability model and the MFD for a city. A model was developed that captures the relation of average velocity and vehicle trip generation in a network, to analytically check the change in average velocity when pooling is introduced. Moreover, a modified shareability model was introduced, which derives further benefits on shareability from an improved average velocity resulting from pooling. Different scenarios were developed for a ride pooling service offered in the city of Munich, where private vehicle trips are substituted by different levels of ride pooling penetration rate ranging from 5%, to 100% (when all the private vehicle trips are substituted by ride pooling vehicle trips). The results show that this analytical model provides a very good and fast estimation of the traffic impacts of ride pooling on the urban environment, requiring only a few input data and the existence of the MFD for a city, which allows for a generalization of a model to other cities, even without the need of network

simulations and calibrations, in cases when MFD is derived analytically or via empirical data (17–20). The analytical model is beneficial for operators to quickly assess the traffic impact of pooling in a certain area of service and for a certain sets of service quality attributes. These insights could be used in discussions with cities to allow or prioritize the operation of such a service.

### Future Work

Future work will include the validation of the developed model for other cities, especially cities with higher levels of congestion in their network, where it could be possible to check if the general assumptions made for this model hold for the congestion regime as well. This would also allow further investigation into whether the assumption used for a parabolic functional form of the MFD is valid for the congestion regime, or if the functional form of the MFD needs to be adjusted to a skewed/asymmetric parabola as in Daganzo, and Laval and Castrillón (16, 20). In addition, the validity of the parameters of the prediction model of shareability (given by Equation 4 and found by data fitting) for other cities is a topic requiring further investigation. Furthermore, the simple model used to derive the reduced number of vehicles resulting from ride pooling based on the shareability will be extended to capture analytically the impact of partially shared trips and how this depends on different optimization objectives used for the matching algorithm. Moreover, the impact of empty vehicle trips generated for passenger pick-ups or re-allocation procedures could also be investigated. The impact of induced demand from other modes, because of increased velocity as a result of ride pooling, is also an interesting topic for further consideration.

### Acknowledgments

The authors would like to thank the anonymous reviewers, whose comments helped in improving the quality of the paper; Florian Dandl and Philipp Franeck for constructive discussions; Gabriel Tilg for sharing his expertise about the MFD; and Majid Rostami for the support with AIMSUN and the calibration of the Munich network.

### Author Contributions

The authors confirm contribution to the paper as follows: study conception and design: A. Bilali, U. Fastenrath, K. Bogenberger; data collection: A. Bilali; analysis and interpretation of results: A. Bilali, U. Fastenrath, K. Bogenberger; draft manuscript preparation: A. Bilali. All authors reviewed the results and approved the final version of the manuscript.


### Declaration of Conflicting Interests


The author(s) declared no potential conflicts of interest with respect to the research, authorship, and/or publication of this article.

### Funding

The author(s) received no financial support for the research, authorship, and/or publication of this article.

### ORCID iDs

Aledia Bilali  <https://orcid.org/0000-0001-7116-7666>

Klaus Bogenberger  <https://orcid.org/0000-0003-3868-9571>

### References

- Mitchell, W. J., C. Borroni-Bird, and L. D. Burns. Reinventing the Automobile. In *Personal Urban Mobility for the 21st Century* (W. J. Mitchell, C. E. Borroni-Bird, and L. D. Burns, eds.), MIT Press, Cambridge, MA, 2010.
- Alonso-Mora, J., S. Samaranayake, A. Wallar, E. Frazzoli, and D. Rus. On-Demand High-Capacity Ride-Sharing via Dynamic Trip-Vehicle Assignment. *Proceedings of the National Academy of Sciences of the United States of America*, Vol. 114, No. 3, 2017, pp. 462–467.
- Fiedler, D., M. Certicky, J. Alonso-Mora, and M. Cap. The Impact of Ridesharing in Mobility-on-Demand Systems: Simulation Case Study in Prague. *Proc., 21st International Conference on Intelligent Transportation Systems (ITSC)*, Maui, HI, IEEE, 2018, pp. 1173–1178.
- Engelhardt, R., F. Dandl, A. Bilali, and K. Bogenberger. Quantifying the Benefits of Autonomous on-Demand Ride-Pooling: A Simulation Study for Munich, Germany. *Proc., IEEE Intelligent Transportation Systems Conference (ITSC)*, Auckland, New Zealand, IEEE, 2019, pp. 2992–2997.
- Krueger, R., T. H. Rashidi, and J. M. Rose. Preferences for Shared Autonomous Vehicles. *Transportation Research Part C: Emerging Technologies*, Vol. 69, 2016, pp. 343–355.
- Santi, P., G. Resta, M. Szell, S. Sobolevsky, S. H. Strogatz, and C. Ratti. Quantifying the Benefits of Vehicle Pooling with Shareability Networks. *Proceedings of the National Academy of Sciences of the United States of America*, Vol. 111, No. 37, 2014, pp. 13290–13294.
- Tachet, R., O. Sagarra, P. Santi, G. Resta, M. Szell, S. H. Strogatz, and C. Ratti. Scaling Law of Urban Ride Sharing. *Scientific Reports*, Vol. 7, 2017, p. 42868.
- Bilali, A., F. Dandl, U. Fastenrath, and K. Bogenberger. Impact of Service Quality Factors on Ride Sharing in Urban Areas. *Proc., 6th International Conference on Models and Technologies for Intelligent Transportation Systems (MT-ITS)*, Cracow, Poland, IEEE, 2019, pp. 1–8.
- Bilali, A., F. Dandl, U. Fastenrath, and K. Bogenberger. An Analytical Model for on-Demand Ride Sharing to Evaluate the Impact of Reservation, Detour and Maximum Waiting Time. *Proc., IEEE Intelligent Transportation Systems Conference (ITSC)*, Auckland, New Zealand, IEEE, 2019, pp. 1715–1720.
- Bilali, A., R. Engelhardt, F. Dandl, U. Fastenrath, and K. Bogenberger. Analytical and Agent-Based Model to Evaluate Ride-Pooling Impact Factors. *Transportation Research Record: Journal of the Transportation Research Board*, 2020. 2674: 1–12.
- Bilali, A., M. A. A. Rathore, U. Fastenrath, and K. Bogenberger. An Analytical Model to Evaluate Traffic Impacts

- of on-Demand Ride Pooling. *Proc., IEEE 23rd International Conference on Intelligent Transportation Systems (ITSC)*, Rhodes, Greece, IEEE, 2020, pp. 1–6.
12. Lehe, L. J., and A. Pandey. Hyperdemand: A Static Traffic Model with Backward-Bending Demand Curves. *Economics of Transportation*, Vol. 24, No. 3, 2020, p. 100182.
  13. Greenshields, B. D. A Study of Traffic Capacity. *Highway Research Board*, Vol. 14, 1935, pp. 448–477.
  14. Godfrey, J. W. The Mechanism of a Road Network. *Traffic Engineering & Control*, Vol. 11, 1969, pp. 323–327.
  15. Cassidy, M. J., K. Jang, and C. F. Daganzo. Macroscopic Fundamental Diagrams for Freeway Networks: Theory and Observation. *Transportation Research Record: Journal of the Transportation Research Board*, 2011. 2260: 8–15.
  16. Daganzo, C. F. Urban Gridlock: Macroscopic Modeling and Mitigation Approaches. *Transportation Research Part B: Methodological*, Vol. 41, No. 1, 2007, pp. 49–62.
  17. Geroliminis, N., and C. F. Daganzo. Existence of Urban-Scale Macroscopic Fundamental Diagrams: Some Experimental Findings. *Transportation Research Part B: Methodological*, Vol. 42, No. 9, 2008, pp. 759–770.
  18. Geroliminis, N., and C. F. Daganzo. Macroscopic Modeling of Traffic in Cities. Presented at 86th Annual Meeting of the Transportation Research Board, Washington, D.C., 2007.
  19. Daganzo, C. F., and N. Gerolim. An Analytical Approximation for the Macroscopic Fundamental Diagram of Urban Traffic. *Transportation Research Part B: Methodological*, Vol. 42, No. 9, 2008, pp. 771–781.
  20. Laval, J. A., and F. Castrillón. Stochastic Approximations for the Macroscopic Fundamental Diagram of Urban Networks. *Transportation Research Part B: Methodological*, Vol. 81, 2015, pp. 904–916.
  21. Luo, Q., and R. Saigal. Dynamic Pricing for on-Demand Ride-Sharing: A Continuous Approach. *SSRN Electronic Journal*, 2017. In *SSRN Journal* 352 (6289), p.1056. DOI: 10.2139/ssrn.3056498.
  22. Ramezani, M., and M. Nourinejad. Dynamic Modeling and Control of Taxi Services in Large-Scale Urban Networks: A Macroscopic Approach. *Transportation Research Part C: Emerging Technologies*, Vol. 94, 2018, pp. 203–219.
  23. Little, J. D. C., and S. C. Graves. Little's Law. In *Building Intuition* (F. S. Hillier, D. Chhajed, and T. J. Lowe, eds.), Springer, Boston, MA, 2008, pp. 81–100.
  24. Ke, J., H. Yang, and Z. Zheng. On Ride-Pooling and Traffic Congestion. *Transportation Research Part B: Methodological*, Vol. 142, No. 9, 2020, pp. 213–231.
  25. Venkateshan, S. P., and P. Swaminathan. Solution of Algebraic Equations. In *Computational Methods in Engineering*. Elsevier, Academic Press, Waltham, 2014, pp. 155–201.
  26. Barceló, J., and J. Casas. Dynamic Network Simulation with AIMSUN. In *Simulation Approaches in Transportation Analysis* (R. Kitamura, and M. Kuwahara, eds.), Springer-Verlag, New York, NY, 2005, pp. 57–98.
  27. Dandl, F., B. Bracher, and K. Bogenberger. Microsimulation of an Autonomous Taxi-System in Munich. *Proc., 5th IEEE International Conference on Models and Technologies for Intelligent Transportation Systems (MT-ITS)*, Naples, Italy, IEEE, 2017, pp. 833–838.
  28. Dandl, F., G. Tilg, M. Rostami-Shahrbabaki, and K. Bogenberger. Network Fundamental Diagram Based Routing of Vehicle Fleets in Dynamic Traffic Simulations. *Proc., IEEE 23rd International Conference on Intelligent Transportation Systems (ITSC)*, Rhodes, Greece, IEEE, 2020, pp. 1–8.
  29. Geroliminis, N., and J. Sun. Hysteresis Phenomena of a Macroscopic Fundamental Diagram in Freeway Networks. *Procedia - Social and Behavioral Sciences*, Vol. 17, No. 1, 2011, pp. 213–228.
  30. Hemdan, S., A. M. Wahaballa, and F. Kurauchi. Quantification of the Hysteresis of Macroscopic Fundamental Diagrams and Its Relationship with the Congestion Heterogeneity and Performance of a Multimodal Network. *Journal of Transportation Technologies*, Vol. 8, No. 1, 2018, pp. 44–64.
  31. Daganzo, C. F., V. V. Gayah, and E. J. Gonzales. Macroscopic Relations of Urban Traffic Variables: Bifurcations, Multivaluedness and Instability. *Transportation Research Part B: Methodological*, Vol. 45, No. 1, 2011, pp. 278–288.

*The authors remain responsible for all findings and opinions presented in the paper.*